



W&M ScholarWorks

Undergraduate Honors Theses

Theses, Dissertations, & Master Projects

5-2017

3-3-1 Models With Unique Lepton Generations and Analysis of Higgs Decays

Karen Ficenec
College of William and Mary

Follow this and additional works at: <https://scholarworks.wm.edu/honorsthesis>

 Part of the [Elementary Particles and Fields and String Theory Commons](#)

Recommended Citation

Ficenec, Karen, "3-3-1 Models With Unique Lepton Generations and Analysis of Higgs Decays" (2017). *Undergraduate Honors Theses*. Paper 1065.
<https://scholarworks.wm.edu/honorsthesis/1065>

This Honors Thesis is brought to you for free and open access by the Theses, Dissertations, & Master Projects at W&M ScholarWorks. It has been accepted for inclusion in Undergraduate Honors Theses by an authorized administrator of W&M ScholarWorks. For more information, please contact scholarworks@wm.edu.

3-3-1 Models With Unique Lepton Generations and Analysis of Higgs Decays

A thesis submitted in partial fulfillment of the requirement
for the degree of Bachelor of Science in Physics from
The College of William and Mary

by

Karen Ficenec

Accepted for

honors



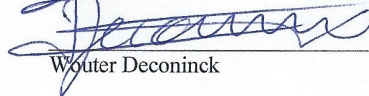
Marc Sher, Director

Gina L. Hoatson

Gina Hoatson, Physics

Rowan Lockwood

Rowan Lockwood



Wouter Deconinck

Williamsburg, VA
April 14, 2017

Contents

1	Abstract	2
2	Motivation	3
3	Introduction	3
3.1	Basics of the Standard Model	3
3.2	The Higgs Mechanism	7
3.3	Anomaly Cancellation	10
4	Models and Results	10
4.1	3-3-1 Models Introduced by Ponce et al.[6]	10
4.2	Overview of 3-3-1 Models by Anderson and Sher [2]	14
4.3	Mass Matrices and Yukawa Couplings	16
4.4	Widths and Branching Ratios	20
4.5	Results: Checking Higgs Decays with Data from the LHC	22
5	Conclusions	28
6	Acknowledgements	29
7	Appendix A: Mathematica Code	30

1 Abstract

We examined several 3-3-1 Models containing three unique lepton generations – each generation has unique quantum numbers and uses the other generations to fully cancel anomalies. These models have been previously discussed in a paper published by Marc Sher and David Anderson [2]. Using new data from the LHC [5], we revisited the Higgs decays presented in these models, and analyzed their viability. Despite the theoretical possibility for extending the Standard Model, none of the models proposed by Anderson and Sher in 2005 have survived experimental verification. We will provide background information on the Standard Model, introduce some of the possible extensions of it, and then show how these extensions failed in comparison to experimental data.

2 Motivation

We seek to find the most accurate model of particles that describes our physical world. The Standard Model of physics describes particles and their interactions using a 3-2-1 Model. 3 and 2 refer to the matrix groups $SU(3)$ and $SU(2)$ and the 1 refers to the unitary $U(1)$ group of complex numbers with modulus 1. The S in $SU(3)$ refers to Special – meaning that overall shifts are controlled for by setting the determinant of the matrices equal to +1 – and the U for Unitary 3x3 matrices that describe the colored quark interactions of QCD [3]. Left-handed lepton and quark flavors interact under the $SU(2) \times U(1)$ group. The $SU(2) \times U(1)$ group breaks down into the electromagnetic and weak interactions. Singlet right-handed quarks and leptons, including electrons, interact under the $U(1)$ group. The spontaneous symmetry breaking of the Higgs, which transforms as an $SU(2)$ doublet, generates the masses of the $SU(2)$ gauge bosons – the W^\pm and Z^0 massive gauge bosons [4]. However, there is nothing restricting these groups to the minimum dimensions which can describe them. For example, the $SU(2)$, 2x2 matrix group, could actually be a subset of a 3x3 space. There are numerous hypotheses that describe such an extension of the standard model. Here, we will examine a few such models in detail and compare with experimental data to verify the probability that these extensions can accurately describe our physical world.

3 Introduction

3.1 Basics of the Standard Model

The Standard Model is created by requiring that the Lagrangian describing particles must be invariant under global and local gauge transformations [3]. The invariance can be thought of in this way: the physical phenomenon which

you describe must be the same wherever you choose your set of axes to be, even if you shift the origin of your coordinate system at each point in space.

By saying that the equation must be invariant using an overall phase shift –global gauge invariance– we find that electric charge must be conserved [3]. Here is an example of a Lagrangian for a free electron (or any free spinor $\frac{1}{2}$ field) [4]:

$$\mathcal{L} = i\bar{\psi}\gamma^\mu\partial_\mu\psi - M\bar{\psi}\psi \quad (1)$$

In this equation, M stands for the mass of the particle, ψ for the wave equation, $\bar{\psi}$ for the antiparticle wave equation, and ∂_μ for the space-time derivative. With this Lagrangian, it is quite simple to show that a global gauge transformation, which can be thought of as an overall phase shift, will not affect the Lagrangian at all. The overall phase shift can be written mathematically as [3]:

$$\psi \rightarrow e^{i\theta}\psi \quad (2)$$

Similarly, for the antiparticle, the phase shift is written as [3]:

$$\bar{\psi} \rightarrow \bar{\psi}e^{-i\theta} \quad (3)$$

Plugging those into the Lagrangian above and simplifying, the original Lagrangian is quickly returned [4].

$$\mathcal{L} = i(\bar{\psi}e^{-i\theta})\gamma^\mu\partial_\mu(e^{i\theta}\psi) - M(\bar{\psi}e^{-i\theta})(e^{i\theta}\psi) \quad (4)$$

$e^{i\theta}$ is a constant in terms of ∂_μ so it can be pulled outside the derivative:

$$\mathcal{L} = (e^{-i\theta}e^{i\theta})i\bar{\psi}\gamma^\mu\partial_\mu\psi - (e^{-i\theta}e^{i\theta})M\bar{\psi}\psi \quad (5)$$

The exponents cancel and the original Lagrangian remains unchanged by the overall phase shift.

$$\mathcal{L} = i\bar{\psi}\gamma^\mu\partial_\mu\psi - M\bar{\psi}\psi \quad (6)$$

This invariance of the Lagrangian under an overall phase shift accurately depicts that the physics must remain unchanged regardless of the coordinate system that we choose. Now we can move on to the more complex local gauge transformation, which mathematically looks like [3]:

$$\psi \rightarrow e^{i\theta(x)}\psi \quad (7)$$

The phase shift θ now has a local, x , dependence. By requiring that the Lagrangian must be invariant under local transformations that vary based on spatial coordinates, we need to adjust the Lagrangian and how it transforms. Because the phase shift of ψ has spatial (x) dependence, the space-time derivative of it will produce an extra term in the Lagrangian due to the product rule of derivatives [4]. This extra term must be accounted for by using a covariant derivative, D_μ [4]:

$$D_\mu = \partial_\mu - ieA_\mu \quad (8)$$

In this equation, A_μ is the field mediator, e is the electric charge, and again, ∂_μ is the space-time derivative [4]. To maintain invariance, this field mediator (the photon for QED, the gluons for QCD) must transform as well, and for QED transforms as [4]:

$$A_\mu \rightarrow A_\mu + \frac{1}{e}\partial_\mu\theta \quad (9)$$

These changes will maintain the invariance of the Lagrangian under local

phase transformations. Because this vector field of photons (A_μ) or gluons is mediated by particles which have energy, it must also contribute a kinetic energy term to the Lagrangian equation (the third term in the equation below) [3]. Therefore, the full Lagrangian for QED has two more terms than the Lagrangians used above with A_μ transforming as described, and $F_{\mu\nu} = \partial_\mu A_\nu - \partial_\nu A_\mu$ [4]:

$$\mathcal{L} = i\bar{\psi}\gamma^\mu\partial_\mu\psi - M\bar{\psi}\psi + \left[\frac{-1}{4}F^{\mu\nu}F_{\mu\nu}\right] - [(q\bar{\psi}\gamma^\mu\psi)A_\mu] \quad (10)$$

By simply requiring that the physical phenomenon described by the Lagrangian remain unchanged by a spatially-dependent shift in coordinate system, we have obtained the full equation describing all of quantum electrodynamics (QED).

The extension to higher dimensions, for example the 3x3 space of quantum chromodynamics, is relatively straightforward, but will include several additional terms because such a space is non-Abelian [4]. First, the phase shift in higher dimensions is described by a set of matrices that create a basis for the space, rather than by a set of real numbers. The phase shift in 3x3 space looks like [4]:

$$\psi \rightarrow e^{i\alpha_a(x)T_a(x)}\psi \quad (11)$$

The T matrices set up a basis for the space, and the α parameters can shift these basis elements [4]. The subscript “a” runs from 1 to 8, and denotes the 8 matrices necessary to set up a basis for the space [3]. Similarly, the covariant derivative, D_μ , now involves these T matrices as well [4]:

$$D_\mu = \partial_\mu + igT_a G_\mu^a \quad (12)$$

For quantum chromodynamics the G_μ^a represents the field mediators, called gluons, and g is the gluon's color charge [4]. There is one more significant change. For real numbers, a and $b \in R$, $ab = ba$. But for matrices that belong to a non-Abelian group, $AB \neq BA$, in other words the matrix group generators do not all commute. This non-commutator relationship between the matrices produces an extra term in the Lagrangian that must be controlled for by altering the way that the gauge bosons transform [3]:

$$G_\mu^a \rightarrow G_\mu^a - \frac{1}{g} \partial_\mu \alpha_a - f_{abc} \alpha_b G_\mu^c \quad (13)$$

f_{abc} are the structure constants of the set of T_α matrices [4]. The compelling result of this transformation of the gauge boson is that the kinetic energy term for the gluons, $G_{\mu\nu}^a G_a^{\mu\nu}$, will now include self-coupling terms in the transformed space [3]. These self-coupling terms lead to confinement of quarks, which is a very exciting and physically accurate result of asserting that local gauge invariance must hold for the QCD Lagrangian.

3.2 The Higgs Mechanism

Correctly describing the transformations of the massless gauge boson fields of photons and gluons is only part of the picture though. The Electroweak interaction adds an interesting complication because it has the massive field mediators known as W^\pm and Z^0 . The masses of these gauge bosons are “hidden” when we approach the electroweak interaction in the same way as the strong and electromagnetic interactions; however, a process called spontaneous symmetry breaking reveals their masses [4].

In spontaneous symmetry breaking, we try to expand a scalar field about a zero value and find that – in the cases where there are massive fields – the zero is not a minimum that we can expand around [3]. The true minima are shifted

at \pm a constant value from the origin. Or in higher dimensions, the minima are at a constant radius from the center of the scalar field [3]. By shifting to these minima, we can then expand the Lagrangian using a perturbative approach that describes quantum energy fluctuations [4]. Once shifted to the actual minima, this expansion will converge and give a realistic answer [4]. Writing the Lagrangian in terms of these new minima introduces a term consistent with a mass term for the gauge bosons. Therefore, this spontaneous symmetry breaking can be used to describe the massive gauge bosons, W^\pm and Z^0 , of the electroweak interaction [3]. Additionally, this new expansion point introduces a massive scalar field. This field is known as the Higgs and is linked to revealing the mass of the electroweak gauge bosons [3].

In the minimal Standard Model approach, there is only one Higgs boson. To get to the Higgs boson, we start by evaluating a scalar ϕ field, expressed as a doublet of complex scalar fields [4]:

$$\phi = \frac{1}{\sqrt{2}} \begin{pmatrix} \phi_1 + i\phi_2 \\ \phi_3 + i\phi_4 \end{pmatrix} \quad (14)$$

The potential, V , of the scalar field in the Lagrangian could look like [4]:

$$V = \mu^2 \phi^\dagger \phi + \lambda (\phi^\dagger \phi)^2 \quad (15)$$

μ represents a constant complex number such that $\mu^2 < 0$ and λ is an arbitrary constant greater than zero [4]. By taking a derivative of V with respect to $\phi^\dagger \phi$ and setting it equal to zero, we find that the minimum is at:

$$\phi^\dagger \phi = -\frac{\mu^2}{2\lambda} \quad (16)$$

By evaluating $\phi^\dagger \phi$, we see that [4]:

$$\phi^\dagger \phi = \frac{1}{2}(\phi_1^2 + \phi_2^2 + \phi_3^2 + \phi_4^2) = -\frac{\mu^2}{2\lambda} \quad (17)$$

Now there is evidently some freedom in our choice of ϕ 's. In the Weinberg-Salam model, we choose [4]:

$$\phi_1 = \phi_2 = \phi_4 = 0 \quad \text{and} \quad \phi_3 = \sqrt{\frac{-\mu^2}{\lambda}} = v \quad (18)$$

The minimum is often denoted v for simplicity. By plugging equation 18 into equation 14, we now have our minimum value of ϕ in 2x2 space, called the vacuum expectation value [4]:

$$\phi_o = \frac{1}{\sqrt{2}} \begin{pmatrix} 0 \\ v \end{pmatrix} \quad (19)$$

and we can expand about this point to describe fluctuations in the Higgs field, $h(x)$:

$$\phi(x) = \frac{1}{\sqrt{2}} \begin{pmatrix} 0 \\ v + h(x) \end{pmatrix} \quad (20)$$

From there, we can obtain the mass terms for the electroweak bosons by plugging the value of ϕ_o into the electroweak Lagrangian [4]. The coefficients of the terms that are negative and have the gauge boson squared define the mass of that gauge boson. The W^\pm masses come out fairly easily, but the W_μ^3 and B_μ have off-diagonal terms [4]. These bosons help set up the basis for the electroweak space, but the actual physical entities of A_μ and Z will diagonalize these matrices. [4] When diagonalizing, Z will come out with a mass and A_μ will come out massless - accurately describing the massless photon field and massive Z boson.

The Standard Model also allows for more Higgs fields, such as a Higgs doublet model, which is analyzed later in this paper.

3.3 Anomaly Cancellation

One way particles can interact with each other is by forming a loop. Analyzing these loops illuminates when a theory is non-renormalizable. Non-renormalizable means having infinities that do not cancel, and as such, the theory is unmanageable. However, by summing over all species that could move through the loop or summing over several generations of quarks or leptons, these anomalies can cancel out; and thus the theory becomes renormalizable again [6].

Anomalies are often presented in tables so that one can add across rows to check that the relevant sums are zero – in other words, that the anomalies are cancelling. This set-up will be used throughout the paper.

4 Models and Results

4.1 3-3-1 Models Introduced by Ponce et al.[6]

Ponce et al. presented several 3-3-1 models [6]. They restricted their models to only include quarks and leptons with non-exotic charges ($\pm \frac{2}{3}$ or $\pm \frac{1}{3}$ for quarks, and ± 1 or 0 for leptons) [6]. Their models included single family and three family models [6]. In single family models, the anomalies individually cancel in each generation. In three family models, we must sum the anomalies over all three generations in order to cancel anomalies [6].

Ponce et al. formed their models by combining different sets of quarks and leptons. I have reproduced a modified version of their anomaly results in the table below followed by a description of each set and its quantum numbers [6]. In some of the descriptions, α stands for an arbitrary generation. For example

ν_α, α^- could stand for ν_e, e^- , namely an electron neutrino and an electron. The first quantum number refers to the color; the colored quarks sets have a 3 here, while the lepton groups - which are colorless - have a 1. The second quantum number references left-handed triplets with a 3 and singlets with a 1. The third quantum number gives the hypercharge. The form of the triplets and their variables will be explained further in the next section.

Anomalies in Ponce et al. 3-3-1 Model fermion sets

Anomalies	L ₁	L ₂	L ₃	L ₄	Q ₁	Q ₂
$[\text{SU}(3)_c]^2\text{U}(1)_X$	0	0	0	0	0	0
$[\text{SU}(3)_L]^2\text{U}(1)_X$	$\frac{-2}{3}$	$\frac{-1}{3}$	0	-1	1	0
$[\text{grav}]^2\text{U}(1)_X$	0	0	0	0	0	0
$[\text{U}(1)_X]^3$	$\frac{10}{9}$	$\frac{8}{9}$	$\frac{6}{9}$	$\frac{12}{9}$	$\frac{-12}{9}$	$\frac{-6}{9}$

$$L_1 = \begin{pmatrix} \nu_\alpha \\ \alpha^- \\ E_\alpha^- \end{pmatrix} \left(1, 3, \frac{-2}{3}\right); \quad \alpha^+ (1, 1, 1); \quad E_\alpha^+ (1, 1, 1) \quad (21)$$

$$L_2 = \begin{pmatrix} \alpha^- \\ \nu_\alpha \\ N_\alpha^0 \end{pmatrix} \left(1, 3^*, \frac{-1}{3}\right); \quad \alpha^+ (1, 1, 1) \quad (22)$$

$$L_3 = \begin{pmatrix} e^- \\ \nu_e \\ N_1^0 \end{pmatrix} \left(1, 3^*, \frac{-1}{3}\right); \begin{pmatrix} E^- \\ N_2^0 \\ N_3^0 \end{pmatrix} \left(1, 3^*, \frac{-1}{3}\right); \begin{pmatrix} N_4^0 \\ E^+ \\ e^+ \end{pmatrix} \left(1, 3^*, \frac{2}{3}\right) \quad (23)$$

$$L_4 = \begin{pmatrix} \nu_e \\ e^- \\ E^- \end{pmatrix} \left(1, 3, \frac{-2}{3}\right); \begin{pmatrix} E_2^+ \\ N_1^0 \\ N_2^0 \end{pmatrix} \left(1, 3, \frac{1}{3}\right); \begin{pmatrix} N_3^0 \\ E_2^- \\ E_3^- \end{pmatrix} \left(1, 3, \frac{-2}{3}\right); \\ e^+ (1, 1, 1); E_1^+ (1, 1, 1); E_3^+ (1, 1, 1) \quad (24)$$

$$Q_1 = \begin{pmatrix} d \\ u \\ U \end{pmatrix} \left(3, 3^*, \frac{1}{3}\right); u^c (3^*, 1, \frac{-2}{3}); d^c (3^*, 1, \frac{1}{3}); U^c (3^*, 1, \frac{-2}{3}) \quad (25)$$

$$Q_2 = \begin{pmatrix} u \\ d \\ D \end{pmatrix} \left(3, 3, 0\right); d^c (3^*, 1, \frac{1}{3}); u^c (3^*, 1, \frac{-2}{3}); D^c (3^*, 1, \frac{1}{3}) \quad (26)$$

An example of a single family model will include one quark (Q) group and one lepton (L) group. For example, the first model presented in this paper was created using group Q_2 and L_3 [6]. If you add columns Q_2 and L_3 , you will get a sum of 0 in each row – this shows that all of the anomalies have cancelled [6]. The first anomaly (the first row in the table) represents two

gluons and a hypercharge. The second one states that the quantum numbers for all left handed interactions must sum to zero. The third anomaly says that the interaction with gravity must produce renormalizable values. Lastly, the anomalies of three interacting singlets (singlets because they are from the U(1) group) must sum to zero. The Feynman diagrams for these anomalies are depicted below.

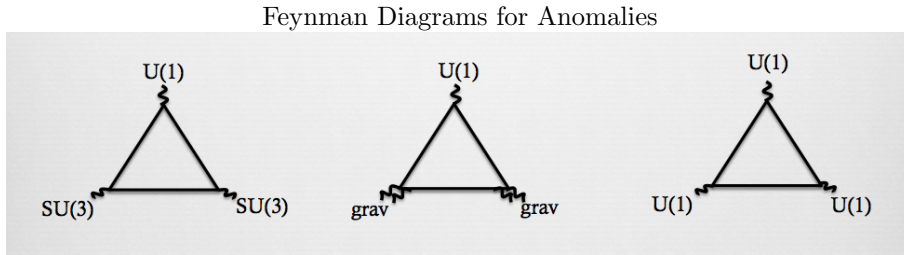


Figure 1: The first diagram represents the first two anomalies in the table. For the first anomaly, the SU(3)'s would be SU(3)_c and for the second anomaly, they would be SU(3)_L. The second diagram shows the third anomaly in the table (grav stands for gravity). And the last Feynman diagram shows the last anomaly in the table regarding U(1) singlets.

We can build up other models by choosing quark (Q_1 or Q_2) and lepton (L_1 , L_2 , L_3 or L_4) groups that sum to have zero anomalies. For example, another one family model will be the combination $Q_1 + L_4$. Three family models presented in the paper include $3L_1 + 2Q_1 + Q_2$ and $3L_2 + Q_1 + 2Q_2$ [6]. The most complex sets discussed were a model composed of $L_1 + L_2 + Q_1 + 2Q_2 + L_3$ and a model of $L_1 + L_2 + 2Q_1 + Q_2 + L_4$ [6]. For these last two models, each family is treated differently [6]. It is simple to check that in all cases, the sum of each of the four anomalies is zero.

As mentioned in the introduction, the SU(2)_L group of the Standard Model relates to the electroweak W^\pm and Z^0 massive gauge bosons. Now that we have expanded the SU(2)_L group to an SU(3)_L group, we have introduced new gauge bosons. Ponce refers to these new gauge bosons as K bosons and D bosons;

there are eight of them [6]. And using spontaneous symmetry breaking, we can find the expected masses of these new gauge bosons.

A few of these models (the last two models mentioned) are explored in more detail by David Anderson and Marc Sher [2].

4.2 Overview of 3-3-1 Models by Anderson and Sher [2]

Anderson and Sher discuss the phenomenology of models $L_1 + L_2 + Q_1 + 2Q_2 + L_3$ called Model A, and $L_1 + L_2 + 2Q_1 + Q_2 + L_4$ called Model B, in which all three generations are treated separately [2]. This is driven by the three unique lepton generations. These are the same models mentioned briefly in the Ponce paper; refer to the Ponce anomaly table to see the related anomalies [6]. Both of these models include exotic leptons. These leptons are not part of the Standard Model and have yet to be observed experimentally. By spontaneous symmetry breaking using Higgs triplets, the mass of these exotic leptons can be discovered. The masses are quite large, explaining why they may not yet have been discovered experimentally [2].

When extending to the $SU(3)_L$ sector, the quark and lepton triplets will have this form [6]:

$$\chi_L = \begin{pmatrix} u \\ d \\ q \end{pmatrix}_L \quad (27)$$

$$\psi_L = \begin{pmatrix} e^- \\ \nu_e \\ \ell \end{pmatrix}_L \quad (28)$$

χ_L stands for the left-handed quark triplets, and ψ_L for the left-handed lepton triplets. The third components, q_L and ℓ_L , are the exotic quarks and

leptons respectively [6].

The leptons of Model A include the electron and neutrino generations of the Standard Model, as well as exotic leptons. When creating new models, we do not know ahead of time what the permutation order of the generations will be, so instead of writing e , μ , and τ , we write e_i , e_j , and e_k and try various permutations when testing the models. The specific leptons in Model A are described (with associated quantum numbers) below [2].

$$\psi_i = \begin{pmatrix} \nu_i \\ e_i \\ E_i \end{pmatrix}_L, (3, \frac{-2}{3}); e_i^c, (1, 1); E_i^c, (1, 1) \quad (29)$$

$$\psi_j = \begin{pmatrix} e_j \\ \nu_j \\ N_j^o \end{pmatrix}_L, (3^*, \frac{-1}{3}); e_j^c, (1, 1) \quad (30)$$

$$\psi_k = \begin{pmatrix} e_k \\ \nu_k \\ N_{1k}^o \end{pmatrix}_L, (3^*, \frac{-1}{3}); \psi'_k = \begin{pmatrix} E_k \\ N_{2k}^o \\ N_{3k}^o \end{pmatrix}_L, (3^*, \frac{-1}{3}); \psi''_k = \begin{pmatrix} N_{4k}^o \\ E_k^c \\ e_k^c \end{pmatrix}_L, (3^*, \frac{2}{3}); \quad (31)$$

The first number in the parenthesis describes whether the particles are in a triplet or a singlet, and the second quantum number denotes the hypercharge. E_i and E_k are the two new exotic charged leptons [2].

Model B is somewhat similar, but has 4 exotic charged leptons rather than three (they are E_i , E_{1k} , E_{2k} and E_{3k}) [2]. All of the leptons in Model B are shown below [2]:

$$\psi_i = \begin{pmatrix} \nu_i \\ e_i \\ E_i \end{pmatrix}_L, (3, \frac{-2}{3}); e_i^c, (1, 1); E_i^c, (1, 1) \quad (32)$$

$$\psi_j = \begin{pmatrix} e_j \\ \nu_j \\ N_j^o \end{pmatrix}_L, (3^*, \frac{-1}{3}); e_j^c, (1, 1) \quad (33)$$

$$\psi_k = \begin{pmatrix} \nu_k \\ e_k \\ E_{1k} \end{pmatrix}_L, (3, \frac{-2}{3}); \psi'_k = \begin{pmatrix} E_{2k}^c \\ N_{1k}^o \\ N_{2k}^o \end{pmatrix}_L, (3, \frac{1}{3}); \quad (34)$$

$$\psi''_k = \begin{pmatrix} N_{3k}^o \\ E_{2k} \\ E_{3k} \end{pmatrix}_L, (3, \frac{-2}{3}); e_k^c, (1, 1); E_{1k}^c, (1, 1); E_{3k}^c, (1, 1) \quad (35)$$

4.3 Mass Matrices and Yukawa Couplings

The Models discussed in this paper have 3 Higgs triplets in their scalar sector. The vacuum expectation values of these Higgs are shown below [2]:

$$\langle \Phi_A \rangle = \begin{pmatrix} 0 \\ 0 \\ V \end{pmatrix}, \quad \langle \Phi_1 \rangle = \begin{pmatrix} \frac{v_1}{\sqrt{2}} \\ 0 \\ 0 \end{pmatrix}, \quad \langle \Phi_2 \rangle = \begin{pmatrix} 0 \\ \frac{v_2}{\sqrt{2}} \\ 0 \end{pmatrix} \quad (36)$$

$\langle \Phi_A \rangle$ breaks the symmetry from $SU(3) \times SU(3) \times SU(1)$ down to the Standard Model symmetry of $3 \times 2 \times 1$ and it gives mass to some of the exotic particles [2]. The $\langle \Phi_1 \rangle$ and $\langle \Phi_2 \rangle$ Higgs break the Standard Model symmetry to adjust to the correct vacuum expectation value and also give mass to the standard model fermions [2]. Because V is much larger than v_1 and v_2 , it will

also cause parts of the mass matrices in Models A and B to decouple, and leave only 3x3 mass matrices in both cases [2].

We will use these 3x3 mass matrices to compute the Yukawa couplings of the Higgs to fermions. We will go through each model separately. The full mass matrix for the charged leptons $(e_i, e_j, e_k, E_i, E_k)$ in model A is shown below, where the h's and g's are arbitrary constants [2]:

$$M_A = \begin{pmatrix} h_1 v_2 & h_2 v_2 & 0 & h_3 v_2 & 0 \\ h_7 v_1 & h_8 v_1 & -g_1 v_2 & h_9 v_1 & g_2 V \\ h_{10} v_1 & h_{11} v_1 & -g_3 v_2 & h_{12} v_1 & g_4 V \\ h_4 V & h_5 V & 0 & h_6 V & 0 \\ h_{13} v_1 & h_{14} v_1 & -g_5 v_2 & h_{15} v_1 & g_6 V \end{pmatrix} \quad (37)$$

As you can see, only the 2 right-most and 2 bottom-most columns involve V. Since v_1 and v_2 are much smaller than V, the upper 3x3 matrix has three zero eigenvalues and completely decouples from the lower region. Non-trivially, based on a numerical calculation performed by Anderson and Sher, the form of the upper 3x3 is maintained [2]. This upper 3x3 then breaks up into its Yukawa Coupling matrices as shown. We changed the numbering system of the h's to make it more readable, since they are just arbitrary coefficients; however, the $v_2 \rightarrow \Phi_2$ and $v_1 \rightarrow \Phi_1$ quality persists when reading off the Yukawa Couplings below from the upper 3x3 in the mass matrix M_A above [2]:

$$\begin{pmatrix} 0 & 0 & 0 \\ h_3 & h_4 & 0 \\ h_6 & h_7 & 0 \end{pmatrix} \Phi_1 + \begin{pmatrix} h_1 & h_2 & 0 \\ 0 & 0 & h_5 \\ 0 & 0 & h_8 \end{pmatrix} \Phi_2 \quad (38)$$

In order to attain Yukawa Couplings with non-arbitrary coefficients, we need to diagonalize the mass matrix [2]. Certain permutations are ruled out, and then we arrive at our usable Yukawa Coupling matrices, as described in Anderson

and Sher's paper [2].

Scalar	A1 (e, μ, τ)	A2 (τ, μ, e)
Φ_1	$\begin{pmatrix} 0 & -\sqrt{m_e m_\mu} & -m_\mu \sqrt{\frac{m_e}{m_\tau}} \\ 0 & -m_\mu & -m_\mu \sqrt{\frac{m_\mu}{m_\tau}} \\ \sqrt{m_e m_\tau} & \sqrt{m_\mu m_\tau} & m_\mu \end{pmatrix}$	$\begin{pmatrix} 0 & 0 & \sqrt{m_e m_\tau} \\ -\sqrt{m_e m_\mu} & -m_\mu & \sqrt{m_\mu m_\tau} \\ -m_\mu \sqrt{\frac{m_e}{m_\tau}} & -m_\mu \sqrt{\frac{m_\mu}{m_\tau}} & m_\mu \end{pmatrix}$
Φ_2	$\begin{pmatrix} m_e & \sqrt{m_e m_\mu} & m_\mu \sqrt{\frac{m_e}{m_\tau}} \\ 0 & 0 & 0 \\ -\sqrt{m_e m_\tau} & -\sqrt{m_\mu m_\tau} & m_\tau + m_\mu \end{pmatrix}$	$\begin{pmatrix} m_e & 0 & -\sqrt{m_e m_\tau} \\ \sqrt{m_e m_\mu} & 0 & -\sqrt{m_\mu m_\tau} \\ m_\mu \sqrt{\frac{m_e}{m_\tau}} & 0 & m_\tau + m_\mu \end{pmatrix}$

m_e stands for the mass of the electron, m_μ for the mass of the muon, and m_τ for the mass of τ . We will pull values from these matrices when computing the formulas for the decay widths (described in the next section).

The procedure for Model B is the same, but we start with a 7x7 matrix (the ordering of charged leptons is: $e_i, e_j, e_k, E_i, E_{1k}, E_{2k}, E_{3k}$) [2].

$$M_B = \begin{pmatrix} h_1 v_2 & h_2 v_2 & h_3 v_2 & h_4 v_2 & h_5 v_2 & g_4 V & h_6 v_2 \\ h_{13} v_1 & h_{14} v_1 & h_{15} v_1 & h_{16} v_1 & h_{17} v_1 & 0 & h_{18} v_1 \\ h_{19} v_2 & h_{20} v_2 & h_{21} v_2 & h_{22} v_2 & h_{23} v_2 & g_5 V & h_{24} v_2 \\ h_7 V & h_8 V & h_9 V & h_{10} V & h_{11} V & -g_1 v_2 & h_{12} V \\ h_{25} V & h_{26} V & h_{27} V & h_{28} V & h_{29} V & -g_2 v_2 & h_{30} V \\ h_{31} v_2 & h_{32} v_2 & h_{33} v_2 & h_{34} v_2 & h_{35} v_2 & g_6 V & h_{36} v_2 \\ h_{37} V & h_{38} V & h_{39} V & h_{40} V & h_{41} V & -g_3 v_2 & h_{42} V \end{pmatrix} \quad (39)$$

Now the lower four rows and right-most four columns contain V's. Again, because V is large, the upper 3x3 will decouple from this lower region, and be used to analyze Standard Model branching ratios and compare them to experiment in the next sections [2]. Maintaining the $v_1 \rightarrow \Phi_1$ and $v_2 \rightarrow \Phi_2$ character in the matrix above, the Yukawa Couplings for Model B for the upper

3x3 are (with the numbering system of the h's changed to make it more readable)

[2]:

$$\begin{pmatrix} 0 & 0 & 0 \\ h'_4 & h'_5 & h'_6 \\ 0 & 0 & 0 \end{pmatrix} \Phi_1 + \begin{pmatrix} h'_1 & h'_2 & h'_3 \\ 0 & 0 & 0 \\ h'_7 & h'_8 & h'_9 \end{pmatrix} \Phi_2 \quad (40)$$

Then, we diagonalize the mass matrix and rewrite the Yukawa Couplings in the correct basis. Showing only allowed permutations, we have 3 options for

Model B [2]:

Scalar	B1 (e, μ , τ)	B2 (e, τ , μ)
Φ_1	$\begin{pmatrix} 0 & -\sqrt{m_e m_\mu} & \sqrt{m_e m_\tau} \\ 0 & -m_\mu & \sqrt{m_\mu m_\tau} \\ 0 & -m_\mu \sqrt{\frac{m_\mu}{m_\tau}} & m_\mu \end{pmatrix}$	$\begin{pmatrix} 0 & 0 & -\sqrt{m_e m_\tau} \\ 0 & 0 & -\sqrt{m_\mu m_\tau} \\ 0 & 0 & m_\tau + m_\mu \end{pmatrix}$
Φ_2	$\begin{pmatrix} m_e & \sqrt{m_e m_\mu} & -\sqrt{m_e m_\tau} \\ 0 & 0 & -\sqrt{m_\mu m_\tau} \\ 0 & 0 & m_\tau + m_\mu \end{pmatrix}$	$\begin{pmatrix} m_e & 0 & -\sqrt{m_e m_\tau} \\ 0 & -m_\mu & \sqrt{m_\mu m_\tau} \\ 0 & -m_\mu \sqrt{\frac{m_\mu}{m_\tau}} & m_\mu \end{pmatrix}$

Scalar	B3 (μ , e, τ)
Φ_1	$\begin{pmatrix} m_e & \sqrt{m_e m_\mu} & m_\mu \sqrt{\frac{m_e}{m_\tau}} \\ 0 & 0 & 0 \\ 0 & 0 & 0 \end{pmatrix}$
Φ_2	$\begin{pmatrix} 0 & \sqrt{m_e m_\mu} & -m_\mu \sqrt{\frac{m_e}{m_\tau}} \\ 0 & -m_\mu & -m_\mu \sqrt{\frac{m_\mu}{m_\tau}} \\ 0 & -m_\mu \sqrt{\frac{m_\mu}{m_\tau}} & m_\tau + 2m_\mu \end{pmatrix}$

4.4 Widths and Branching Ratios

The Higgs boson can decay into other particles. The branching ratio gives the probability of a Higgs decaying into a given pair of particles. This probability is then multiplied by the total decay width to get the width of the decay into the given pair of particles called Γ_{xx} :

$$\Gamma_{xx} = \text{SMBranchingRatio}_{xx} * \Gamma_{Total} \quad (41)$$

The Standard Model branching ratios with error are shown [1]:

Theoretical Standard Model Branching Ratios [1]

Higgs Decay into	Branching Ratio (%)
$\tau\tau$	6.26 ± 0.35
$\mu\mu$	0.022 ± 0.001
WW*	22.0 ± 0.9
ZZ*	2.73 ± 0.11
$b\bar{b}$	57.1 ± 1.9
gg	8.53 ± 0.85

Using these branching ratios and the total decay width of 4.1 MeV from the ATLAS experiment [1], I calculated the individual decay widths into $\tau\tau$, $\mu\mu$, WW, ZZ, bb, and gg; they are:

Standard Model Decay Widths

$\Gamma_{\tau\tau} = 0.2567 \text{ MeV}$
$\Gamma_{\mu\mu} = 0.000902$
$\Gamma_{ww} = 0.902$
$\Gamma_{zz} = 0.1119$
$\Gamma_{bb} = 2.3411$
$\Gamma_{gg} = 0.3497$

In order to find the decay widths of our models, we need to multiply by the squared Yukawa Coupling. Using the Yukawa Coupling matrices in the previous section, I found expressions for how strongly the Higgs couples to each particle. In order to calculate the coupling constants, I wrote the Higgs that breaks the SM symmetry in the models (called h), in terms of its mixing with the exotic $\langle\Phi_A\rangle$ Higgs. With α as the mixing angle, that equality is:

$$h = \phi_1 \sin(\alpha) - \phi_2 \cos(\alpha) \tag{42}$$

The ϕ_1 is then replaced with the particle's coupling to the ϕ_1 from the Yukawa coupling matrices (and likewise for ϕ_2). For example, in model A1, the ϕ_1 coupling to $\tau\tau$ would be m_μ - taken directly from the $\tau\tau$ or (3,3) place in the A1, ϕ_1 coupling matrix. Replacing v_1 and v_2 with $v \cos(\beta)$ and $v \sin(\beta)$ respectively, I wrote them in terms of the common ratio of SM higgs:

$$\tan(\beta) = \frac{v_2}{v_1} \tag{43}$$

After entering the ϕ_1 and ϕ_2 values into the h equation, I squared it, and multiplied by the Standard Model width for that particle; this created the approximate decay widths for each particle in each model. The decay widths are

shown explicitly for each model in the next section. Within each model, I determined the branching ratio by putting an individual decay width over the sum of all other decay widths.

$$BR_{xx} = \frac{\Gamma_{xx}}{\Sigma\Gamma_{xx}} \quad (44)$$

These Branching Ratios are then compared to experimental values. The experimental branching ratios are shown in the table below [5]. When graphing the branching ratios, I used twice the error bounds given (two standard deviations) for upper and lower limits.

Experimental Branching Ratios in percentages (%) [5]

$\Gamma_{\tau\tau} = 7.011 \pm 1.44$
$\Gamma_{\mu\mu} < 0.154$
$\Gamma_{ww} = 23.76 \pm 3.74$
$\Gamma_{zz} = 3.522 \pm 0.669$
$\Gamma_{bb} = 46.822 \pm 17.13$

4.5 Results: Checking Higgs Decays with Data from the LHC

I will now compare the experimental decay branching ratios to the branching ratios predicted by each allowed permutation of model A and B. The branching ratio is obtained by putting a single decay width over the sum of all decay widths. Refer to the section above to see how the decay widths below were obtained. For Model A1 the decay widths are as follows:

$$\Gamma_{\tau\tau} = (0.2567 \text{ MeV}) \left[\left(\frac{\sqrt{2} m_\tau}{v} \right) \left(\frac{m_\mu \sin(\alpha)}{m_\tau \cos(\beta)} - \left(\frac{m_\mu + m_\tau}{m_\tau} \right) \frac{\cos(\alpha)}{\sin(\beta)} \right) \right]^2 \quad (45)$$

$$\Gamma_{\mu\mu} = (9.02 \times 10^{-4} \text{ MeV}) \left[\left(\frac{\sqrt{2} m_\mu}{v} \right) \frac{\sin(\alpha)}{\cos(\beta)} \right]^2 \quad (46)$$

$$\Gamma_{ww} = (0.902 \text{ MeV}) \sin^2(\alpha - \beta) \quad (47)$$

$$\Gamma_{zz} = (0.1119 \text{ MeV}) \sin^2(\alpha - \beta) \quad (48)$$

$$\Gamma_{bb} = (2.3411 \text{ MeV}) \left[\left(\frac{\sqrt{2} m_\tau}{v} \right) \left(\frac{m_\mu \sin(\alpha)}{m_\tau \cos(\beta)} - \left(\frac{m_\mu + m_\tau}{m_\tau} \right) \frac{\cos(\alpha)}{\sin(\beta)} \right) \right]^2 * 25 \sin^2(\alpha) \quad (49)$$

$$\Gamma_{gg} \approx 0.3497 \text{ MeV} \quad (50)$$

The decay widths for WW, ZZ, and gg are equal to the A1 model values for all other models discussed in this paper, because these gauge bosons are the same in all of the models.

For Model A2, the decay width for $\tau\tau$ and bb depend on the ratio of the electron mass over the vacuum expectation value $\left(\frac{\sqrt{2} m_e}{v}\right)$ which is 0.5 MeV over 175 Gev; therefore, these decay widths are approximately zero. Again, the WW, ZZ, and gg widths are equal to those shown for A1. For Model A2, the $\mu\mu$ width is equal to that in model A1 as well:

$$\Gamma_{\mu\mu} = (9.02 \times 10^{-4} \text{ MeV}) \left[\left(\frac{\sqrt{2} m_\mu}{v} \right) \frac{\sin(\alpha)}{\cos(\beta)} \right]^2 \quad (51)$$

In Model B1, the decay widths for $\tau\tau$, $\mu\mu$, WW, ZZ, and gg are all the same as Model A1; however, the decay width for bb is larger by a factor of 400 over 25:

$$\Gamma_{bb} = (2.3411 \text{ MeV}) \left[\left(\frac{\sqrt{2} m_\tau}{v} \right) \left(\frac{m_\mu \sin(\alpha)}{m_\tau \cos(\beta)} - \left(\frac{m_\mu + m_\tau}{m_\tau} \right) \frac{\cos(\alpha)}{\sin(\beta)} \right) \right]^2 * 400 \sin^2(\alpha) \quad (52)$$

For Model B2, WW, ZZ, and gg are the same as Model A1, and the other decay widths are shown below:

$$\Gamma_{\tau\tau} = (0.2567 \text{ MeV}) \left[\left(\frac{\sqrt{2} m_\mu}{v} \right) \frac{\cos(\alpha)}{\sin(\beta)} \right]^2 \quad (53)$$

$$\Gamma_{\mu\mu} = (9.02 \times 10^{-4} \text{ MeV}) \left[\left(\frac{\sqrt{2} m_\tau}{v} \right) \left(\left(\frac{m_\mu + m_\tau}{m_\tau} \right) \frac{\sin(\alpha)}{\cos(\beta)} - \frac{m_\mu \cos(\alpha)}{m_\tau \sin(\beta)} \right) \right]^2 \quad (54)$$

$$\Gamma_{bb} = (2.3411 \text{ MeV}) \left[\left(\frac{\sqrt{2} m_\mu}{v} \right) \frac{\cos(\alpha)}{\sin(\beta)} \right]^2 * 25 \sin^2(\alpha) \quad (55)$$

Lastly, for Model B3 - WW, ZZ, and gg are the same as in Model A1. The $\mu\mu$ decay width is essentially zero, because it depends on the electron mass over 175 GeV. The $\tau\tau$ and bb widths are shown below:

$$\Gamma_{\tau\tau} = (0.2567 \text{ MeV}) \left[\left(\frac{\sqrt{2}(m_\tau + 2 m_\mu)}{v} \right) \frac{\cos(\alpha)}{\sin(\beta)} \right]^2 \quad (56)$$

$$\Gamma_{bb} = (2.3411 \text{ MeV}) \left[\left(\frac{\sqrt{2}(m_\tau + 2 m_\mu)}{v} \right) \frac{\cos(\alpha)}{\sin(\beta)} \right]^2 * 1000 \sin^2(\alpha) \quad (57)$$

In each model, I used the expression below to calculate the branching ratios for each particle:

$$BR_{xx} = \frac{\Gamma_{xx}}{\Sigma\Gamma_{xx}} \quad (58)$$

The model branching ratios still have the free parameters of α - mixing angle, and β - inverse tangent of v_2 to v_1 . I set the model branching ratios equal to the branching ratios found experimentally $\pm 2x$ the error bounds, and plotted the results to see if any of the models' branching ratios agreed with experiment.

While there was a range of alpha and beta values that worked for the branching ratios of Higgs into WW bosons in most models, there often were no α and β values satisfying $\tau\tau$ decay in these models. The real solutions for $\tau\tau$ branching tended to be outside the allowed range. They were either too small, $\tan(\beta) < 1$, in which case the perturbation theory no longer applies; or they were too large, $\tan(\beta) > 100$, in which case the Higgs would not be able to give the necessary mass to bottom or top quarks. In each model, the $\tau\tau$ decay had no α and β values in range; therefore, each of the theories were eliminated. A2 was eliminated most easily, because it predicted no $\tau\tau$ decay, even though that decay is observed experimentally. I have included some example graphs of the WW Branching ratios below, which did have some allowed values as shown. (The code for generating these graphs is shown in Appendix A.)

WW Branching in Model A1

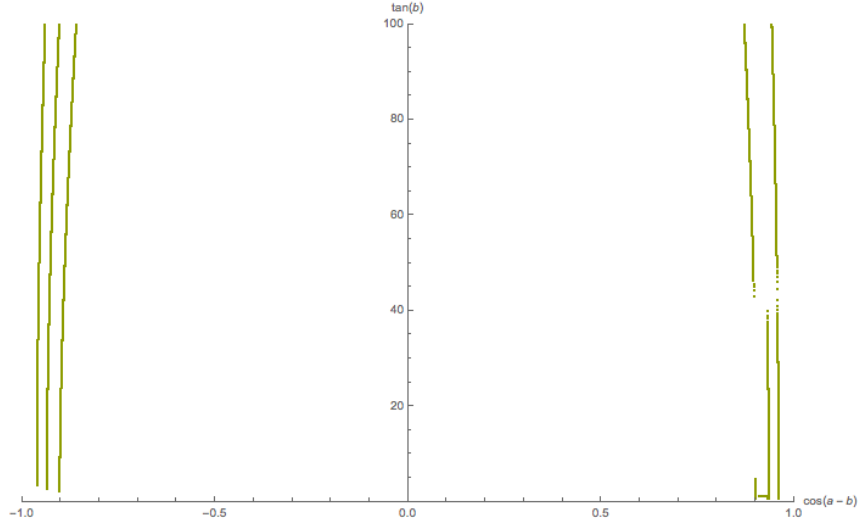


Figure 2: In terms of $\cos(\alpha - \beta)$ on the horizontal axis and $\tan(\beta)$ on the vertical axis, this graph shows the α and β angles that satisfy both the branching ratios of Model A1 and the experimental results about the branching ratio of the Higgs into the WW bosons. The three lines represent the main solution and the upper and lower bounds (at two standard deviations of the experimental values). The graph does not appear exactly symmetric. This may be due to the complex branching ratio equation only being satisfied by certain values as α runs from $-\pi/2$ to $\pi/2$ and β runs from 0 to π .

WW Branching in Model B1

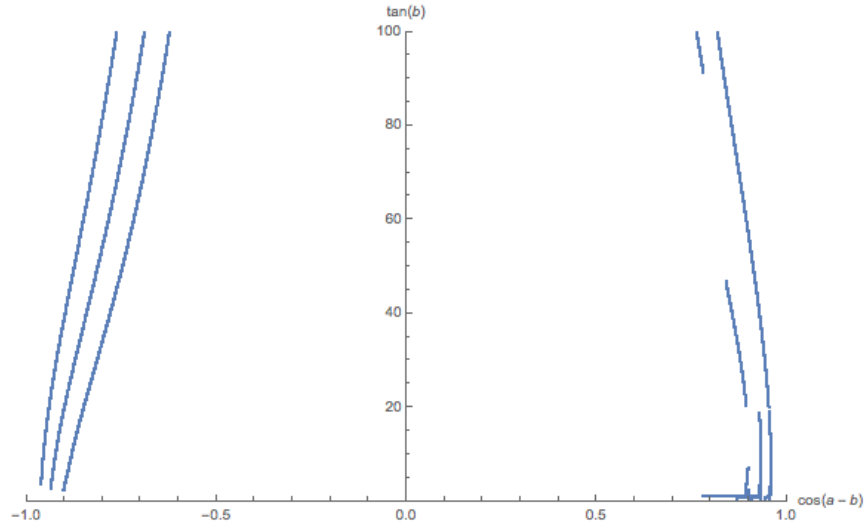


Figure 3: In terms of $\cos(\alpha - \beta)$ and $\tan(\beta)$, this graph shows the α and β angles that satisfy both the branching ratios of Model B1 and the experimental results about the branching ratio of the Higgs into the WW bosons. The three lines represent the main solution and the upper and lower bounds (at two standard deviations of the experimental values). The graph does not appear exactly symmetric. This may be due to the complex branching ratio equation only being satisfied by certain values as α runs from $-\pi/2$ to $\pi/2$ and β runs from 0 to π .

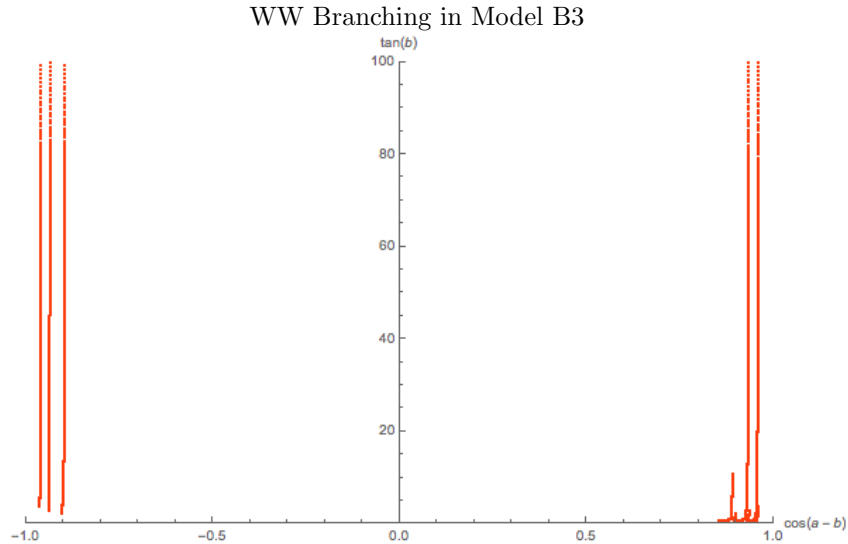


Figure 4: In terms of $\cos(\alpha - \beta)$ and $\tan(\beta)$, this graph shows the α and β angles that satisfy both the branching ratios of Model B3 and the experimental results about the branching ratio of the Higgs into the WW bosons.

5 Conclusions

We examined a 3-3-1 extension of the $SU(2) \times U(1)$ group in the Standard Model. Our theories involved 3 unique lepton generations, large exotic quark and lepton masses, and 3 Higgs triplets. The Higgs particles in the models had some interesting decay states with large branching ratios, but these did not agree with experimental bounds on the branching ratios for the Higgs Boson. Contrary to experiment, Model A2 had no $\tau\tau$ decay because the Yukawa Coupling was dependent on the small ratio of m_e over $\frac{v}{\sqrt{2}}$ or 0.0000029; so it was discarded. In Models A1, B1, B2, and B3 the $\tau\tau$ decay had no mixing angle α and no vacuum expectation value ratio $\tan(\beta)$ that were within the range of allowed values and agreed with experimental data. All the models hypothesized by Anderson and Sher in 2005 have been disproven using more recent experimental data from

the LHC [5]. Perhaps other extensions of the Standard Model will hold up to experimental scrutiny.

6 Acknowledgements

I would like to thank my adviser Marc Sher for answering the many questions that I developed while learning about the Standard Model and its extensions. I would also like to thank professors Rossi and Deconinck for augmenting my general understanding of physics through insightful discussions. And professors Lockwood, Vahle and Harbron for their extraordinary teaching skills.

7 Appendix A: Mathematica Code

Note: The code is functional but not efficient.

Code for Graphing WW: Part 1

```
Clear["Global *"];
Clear[blist];
Clear[blistfirst];
Clear[ffirst]; Clear[gfirst]; Clear[pfirst];
Clear[blistsec]; Clear[fsec]; Clear[gsec]; Clear[psec];
Clear[blistthird]; Clear[fthird]; Clear[gthird]; Clear[pthird];
Clear[blist];
Clear[blistfirst];
Clear[flfirst];
Clear[glfirst];
Clear[plfirst];
Clear[blistsec];
Clear[flsec];
Clear[glsec];
Clear[plsec];
Clear[blistthird];
Clear[fthird];
Clear[glthird];
Clear[plthird];
Clear[bhlist];
Clear[bhlistfirst];
Clear[fhfirst];
Clear[ghfirst];
Clear[pfirst];
Clear[bhlistsec];
Clear[fhsec];
Clear[ghsec];
Clear[psec];
Clear[bhlistthird];
Clear[fhthird];
Clear[ghthird];
Clear[pthird];
```

Figure 5: This section of the code addresses a troubleshooting issue. The saved global variables had to be cleared at the beginning of each run in order to not have leftover (incorrect) variable values.

Code for Graphing WW: Part 2

```

Clear[pthird];
fullList = List[];
For[a = -(Pi/2), a < (Pi/2), (a = a + 0.0001),
  q = Solve[(1/0.2376) * 0.902 * ((Sin[a - b]) ^ 2) ==
    0.25666 *
      (((105.66 / 175 000) * (Sin[a] / Cos[b]) -
        (1776.82 / 175 000) * (Cos[a] / Sin[b])) ^ 2) +
      0.000902 * (((105.66 / 175 000) * (Sin[a] / Cos[b])) ^ 2) +
      0.902 * ((Sin[a - b]) ^ 2) + 0.11193 * ((Sin[a - b]) ^ 2) +
      2.3411 *
      (((105.66 / 175 000) * (Sin[a] / Cos[b]) -
        (1776.82 / 175 000) * (Cos[a] / Sin[b])) * Sin[a] * 5) ^
      2) + 0.34973, b];
blist = (N@(b + 0) /. q);
blist = Select[blist, Element[#, Reals] &];
blist = Select[blist, (0 < # < Pi) &];
blist = Select[blist, (0.5 < Tan[#] < 100) &];
If[Length[blist] > 0, blistfirst = First[blist];
  ffirst = (N@Tan[blistfirst]);
  gfirst = (N@Cos[a + -blistfirst]);
  pfirst = {gfirst, ffirst}];
If[(Length[blist] > 1), blistsec = Part[blist, 2];
  fsec = (N@Tan[blistsec]);
  gsec = (N@Cos[a + -blistsec]);
  psec = {gsec, fsec}];
If[Length[blist] > 2, blistthird = Part[blist, 3];
  fthird = (N@Tan[blistthird]);
  gthird = (N@Cos[a + -blistthird]);
  pthird = {gthird, gfirst}];

```

Figure 6: The first line is the last clear command from figure 5. The second line sets up a list, called “fullList” that is filled in the code segment shown in figure 8 to collect all data points. The third line begins a for loop that runs through possible α values, using a small increment of 0.0001. The q variable will return the β values that satisfy the branching ratio expression when it is set equal to the experimental branching ratio. blist makes a list of all the β solutions. I then stripped off any imaginary numbers in this list, and selected only the allowed values of β (between 0 and Pi). Next, I removed any values for which $\tan(\beta)$ was less than 0.5 or greater than 100. From checking the solutions “by hand” (see figure 9), I knew that there were no more than 3 solutions for β after this stripping process. In fact, there were sometimes no solutions. Therefore, I used conditional if statements to check the length of the list of β solutions. If the list had a value in it, I saved the value (as blistfirst), as well as tangent of the value, and $\cos(\alpha-\beta)$, and made a point for the graph (called pfirst). The final lines of this code segment repeat that process for any possible second and third solutions.

Code for Graphing WW: Part 3

```

pthird = {gthird, gfirst}];
ql = Solve[(1/0.1628)*0.902*((Sin[a - bl])^2) ==
0.25666*
(((105.66/175000)*(Sin[a]/Cos[bl]) -
(1776.82/175000)*(Cos[a]/Sin[bl]))^2) +
0.000902*(((105.66/175000)*(Sin[a]/Cos[bl]))^2) +
0.902*((Sin[a - bl])^2) + 0.11193*((Sin[a - bl])^2) +
2.34111*
(((105.66/175000)*(Sin[a]/Cos[bl]) -
(1776.82/175000)*(Cos[a]/Sin[bl]))*Sin[a] + 5)^
2) + 0.34973, bl];
bllist = (N@(bl + 0) /. ql);
bllist = Select[bllist, Element[#, Reals] &];
bllist = Select[bllist, (0 < # < Pi) &];
bllist = Select[bllist, (0.5 < Tan[#] < 100) &];
If[Length[bllist] > 0, bllistfirst = First[bllist];
flfirst = (N@Tan[bllistfirst]);
glfirst = (N@Cos[a + -bllistfirst]);
plfirst = {glfirst, flfirst}];
If[Length[bllist] > 1, bllistsec = N@Part[bllist, 2];
flsec = (N@Tan[bllistsec]);
glsec = (N@Cos[a + -bllistsec]);
plsec = {glsec, flsec}];
If[Length[bllist] > 2, bllistthird = Part[bllist, 3];
flthird = (N@Tan[bllistthird]);
glthird = (N@Cos[a + -bllistthird]);
plthird = {glthird, flthird}];

```

Figure 7: This code segment again finds β solutions, makes and cleans a list of those solutions, and saves points; however, this time, it solves for the lower experimental bound, and all the variables have an extra l to indicate this lower bound.

Code for Graphing WW: Part 4

```

plthird = {glthird, flthird}];
qh = Solve[(1/0.3124)*0.902*((Sin[a - bh])^2) ==
0.25666 *
(((105.66/175000)*(Sin[a]/Cos[bh]) -
(1776.82/175000)*(Cos[a]/Sin[bh]))^2) +
0.000902*(((105.66/175000)*(Sin[a]/Cos[bh]))^2) +
0.902*((Sin[a - bh])^2) + 0.11193*((Sin[a - bh])^2) +
2.3411 *
((((105.66/175000)*(Sin[a]/Cos[bh]) -
(1776.82/175000)*(Cos[a]/Sin[bh]))*Sin[a]*5)^
2) + 0.34973, bh];
bhlist = (N@(bh + 0) /. qh);
bhlist = Select[bhlist, Element[#, Reals] &];
bhlist = Select[bhlist, (0 < # < Pi) &];
bhlist = Select[bhlist, (0.5 < Tan[#] < 100) &];
If[Length[bhlist] > 0, bhlistfirst = First[bhlist];
fhfirst = (N@Tan[bhlistfirst]);
ghfirst = (N@Cos[a + -bhlistfirst]);
phfirst = {ghfirst, fhfirst}];
If[Length[bhlist] > 1, bhlistsec = Part[bhlist, 2];
fhsec = (N@Tan[bhlistsec]);
ghsec = (N@Cos[a + -bhlistsec]);
phsec = {ghsec, fhsec}];
If[Length[bhlist] > 2, bhlistthird = Part[bhlist, 3];
fhthird = (N@Tan[bhlistthird]);
ghthird = (N@Cos[a + -bhlistthird]);
phthird = {ghthird, fhthird}];
If[Length[bhlist] > 0, fullList = Append[fullList, pfirst]];
If[Length[bhlist] > 1, fullList = Append[fullList, psec]];
If[Length[bhlist] > 2, fullList = Append[fullList, pthird]];
If[Length[bhlist] > 0, fullList = Append[fullList, plfirst]];
If[Length[bhlist] > 1, fullList = Append[fullList, plsec]];
If[Length[bhlist] > 2, fullList = Append[fullList, plthird]];
If[Length[bhlist] > 0, fullList = Append[fullList, phfirst]];
If[Length[bhlist] > 1, fullList = Append[fullList, phsec]];
If[Length[bhlist] > 2, fullList = Append[fullList, phthird]];
Clear[a];
ListPlot[fullList, PlotRange -> {{-1, 1}, {0, 100}},
AxesLabel -> {Cos[a - b], Tan[b]}]

```

Figure 8: This code segment again finds β values, makes a list, and saves points (this time for the upper bound, indicated with an “h” for high). Additionally, in this code segment, I added any points to a “fullList”, from which Mathematica could plot all the points. In order to not have empty lists filling up the fullList, I used conditionals to only add actual solutions to the fullList. The for loop then closed; and once outside the for loop, I plotted all these solution points to make the graphs.

```

Code for Checking  $\tau\tau$  "By Hand"
For[a = -(Pi/2), a < (Pi/2), {a = a + 0.001},
k =
Solve[
(1/0.098908) * 0.2583 *
(((105.66/175000) * (Sin[a]/Cos[b]) -
(1776.82/175000) * (Cos[a]/Sin[b])) ^ 2) ==
0.2583 *
(((105.66/175000) * (Sin[a]/Cos[b]) -
(1776.82/175000) * (Cos[a]/Sin[b])) ^ 2) +
0.000861 * (((105.66/175000) * (Sin[a]/Cos[b])) ^ 2) +
0.861 * ((Sin[a - b]) ^ 2) + 0.1107 * ((Sin[a - b]) ^ 2) +
2.378 *
((((105.66/175000) * (Sin[a]/Cos[b]) -
(1776.82/175000) * (Cos[a]/Sin[b])) * Sin[a] + 5) ^ 2) +
0.3362, b];
klist = (N@(b + 0) /. k);
klist = Select[klist, Element[#, Reals] &];
klist = Select[klist, (0 < # < Pi) &];
klist = Select[klist, (0.5 < Tan[#] < 150) &];
Print[klist]]

```

Figure 9: This code is essentially one of the code segments shown above (for either the main solution, or the upper or lower bound). I could adjust the bound by hand in this code, to check different solutions in the error range. The Print statement is shown here at the end of the selection process, but when checking by hand, I moved it in between all selection items to check that the code was performing as desired. (For example I inserted the Print before the Reals selection and checked that none of the imaginary values were just 0.00000001i, but actually had a large i component.) As you can see, I also altered the range of $\tan(\beta)$ up to 150, to make sure that no solutions lay just out of range. For $\tau\tau$ graphing, I got only a blank graph, so I used this code to make sure that the code was working properly and there really were no solutions.

References

- [1] Georges Aad et al. “Measurements of the Higgs boson production and decay rates and coupling strengths using pp collision data at $\sqrt{s} = 7$ and 8 TeV in the ATLAS experiment”. In: *Eur. Phys. J. C*76.1 (2016), p. 6. DOI: 10.1140/epjc/s10052-015-3769-y. arXiv: 1507.04548 [hep-ex].
- [2] David L. Anderson and Marc Sher. “3-3-1 Models with Unique Lepton Generations”. In: *Physical Review* 72.9 (2005). DOI: 10.1103/PhysRevD.72.095014.
- [3] David Griffiths. *Introduction to Elementary Particles*. New York: Harper Row Publishers, 1987. ISBN: 0-06-042513-X.
- [4] Francis Halzen and Alan D. Martin. *Quarks Leptons: An Introductory Course in Modern Particle Physics*. John Wiley Sons, Inc., 1984. ISBN: 0-471-88741-2.
- [5] C. Patrignani et al. “Gauge and Higgs Bosons”. In: *Chin. Phys.* C40 (2016), p. 100001.
- [6] William A. Ponce, Juan B. Florez, and Luis A. Sanchez. “Analysis of SU(3)(c) x SU(3)(L) x U(1)(X) local gauge theory”. In: *Int. J. Mod. Phys. A*17 (2002), pp. 643–660. DOI: 10.1142/S0217751X02005815. arXiv: hep-ph/0103100 [hep-ph].